

STRUCTURAL CAPACITY OF NSM STEEL BARS STRENGTHENED DEEP BEAMS UNDER COMBINED LOADS OF REPEATED AND ELEVATED TEMPERATURE

*Aula H. Faeq¹Ali H. Aziz¹

1) Civil Engineering Department, College of Engineering, Mustansiriyah University, Baghdad, Iraq

Received 14/5/2021

Accepted in revised form 2/7/2021

Published 1/11/2021

Abstract: The current experimental investigation is devoted to study the structural capacity of near-surface mounted steel bars strengthened deep beams. Six reinforced SCC deep beam specimens with a dimension of 1400mm x175mm x350mm were tested under Combined Loads of Repeated and Elevated Temperature. The adopted variable includes the type of loading, degree of elevated temperature, and presence or absence of the strengthening by NSM-steel bars. The experimental results show that the ultimate load of B2-R-T20 decreased by about 33% when the applied load changed from monotonic to repeated; also, when the degree of burning increased to (200°C) and (350°C), the ultimate load decreased by 44% and 65%, respectively. The presence of the strengthened NSM-steel bars leads to increase the lateral strength of the tested beams and arrested the diagonal cracks to be widening as a result, the ultimate load capacity increases by (193%-197%) for the samples exposed to elevated temperature, in comparison with reference beams. The adopted strengthened technique proved to be adequate to restore and increase the shear capacity of the tested beams.

Keywords: Deep Beam, Self-Compacting Concrete, NSM, Elevated Temperature, Repeated Load.

1. Introduction

Reinforced concrete deep beams with a small span-to-depth ratio are commonly used as transfer girders in several structural applications such as buildings, bridges, and offshore

structures. Since the significant proportion of the deep beam load is transferred directly to the support, through a single strut, shear rather than flexural strength is usually controlled. On the other extreme, its shear intensity is considerably higher than that expected by slender beams expressions. As a result, special design methods are required to account for these differences. Two-dimensional elasticity techniques can be used to investigate stresses in deep beams prior to cracking. These studies show that plane sections before bending do not always remain plane after bending, particularly when severe cross-section warping occurs due to high shear stresses. As a consequence, even in the elastic range, flexural stresses are not linearly distributed, and conventional methods for calculating section properties and stresses cannot be used [1].

Because of the unique behavior of deep beams, some codes, such as the ACI-318 Code [2] and the Canadian Code (CSA) [3], provide design guidance, whereas other codes or standards, such

*Corresponding Author: aula.alsaffar@yahoo.com

as the British standards (BS8110) [4], do not [5, 6].

The change in structural members loading, function, errors in design or construction, and deterioration of interior elements, such as corrosion of steel reinforcement, due to environmental factors, require an increase or restore to the load capacity, as a result, the member should be strengthened by using adequate technique. The Increase in deep beams strength is attainable by using different techniques such as externally strengthening by steel plates, CFRP strips, prestressing strand and utilization of special types of concrete (HSC, SFRC, RPC....). Fiber reinforced polymer (FRP) materials in general, and bars in particular, are commercially available in many applications. Conventional steel bars can provide reinforcement for NSM strengthening in structural elements where corrosion is not a threat or where external corrosion protection can be applied. Although the using of NSM reinforcement for strengthening is not a modern technique, but at the other hand, steel bars are readily available, cheaper, show sufficient ductility (long-term ductility) and bond performance [7].

The overcrowding of rebar's in reinforced concrete (RC) members such as columns and deep beams makes proper concrete compacting with a mechanical vibrator impossible. Unfilled voids and macro-pores in concrete caused by improper vibration and compaction can compromise the concrete's mechanical strength and toughness, and are one of the leading causes of concrete deterioration [8]; therefore, self-compacting concrete could be used to make element construction efficient while maintaining structural performance and durability.

During the normal traffic flow (passage of vehicles) of the bridges, dynamic excitations

(traffic-vibrations) are generated in a certain level. The vibration and the levels of dynamic responses should be considered in design. One way to take into account the dynamic response is a repeated loading.

The analysis of deep beam behavior is a major topic in research on reinforced concrete structures. In 2002, Aguilar et al [9] studied the monotonic test of four simply supported beam specimens; the performance and strength of reinforced concrete deep beams were carried out. The tested beams were made with (28MPa) concrete compressive strength and dimensions of 4470x915x305mm. The primary adopted parameters were the horizontal and vertical shear reinforcement ratios. The main test results were compared with the results of the ACI318-99 Code [10] equations and the strut and tie model (STM) approach adopted by the ACI318-11 Code [2]. They noticed that in the flexural compression zone close the loading plate, all specimens showed diagonal cracks and some crushing of concrete at failure. Two of the specimens with efficient horizontal shear reinforcement failed by flexure, while two other specimens failed by shear compression, reinforced by a limited amount of horizontal shear reinforcements. The STM model provides better representation and results in a reduction in the amount of vertical and horizontal shear reinforcement needed.

Heiza, et.al (2012) (2012) [11] investigated the shear strengthening technique for deep beams. The deep beams of reinforced self-compacting concrete (RSCC) were proposed and compared to some traditional techniques. Sixteen RSCC deep beams with constant cross-section of 1200 x500mm and effective span of 1000 mm were tested. Fifteen beam specimens were cast with 200x200mm central openings, while the last beam was cast without openings and considered as a reference beam. Two different techniques,

externally bonded layers (EBL) and near-surface mounted reinforcement (NSMR), with various materials such as steel, carbon and glass fiber reinforced polymers (CFRP and GFRP) were executed. Based on the anchorage length of GFRP rods, the latest technique for shear strengthening improves the load capacity by about 36-55%. In order to study more thoroughly the structural behavior of the tested beams, two-dimensional nonlinear finite elements analysis was used. The analytical findings were very similar to the results of the experiment.

Mohamad, et.al (2015) [12] investigate the behavior and load ability of reinforced concrete strengthened and repaired with carbon fiber reinforced polymer (CFRP) rods in shear. The study focused in how the orientation and spacing of CFRP rods influence the shear conduct and load carrying capacity for NSM beams designed for shear failure. The research program consists of produce and test of five simply supported reinforced concrete deep beam specimens with dimensions of 1300x150x400mm, made with concrete compressive strength of (31MPa) at 28 days. The tested beams were designed to be failed in shear and strengthened by NSM-CFRP rods. The findings indicate that the externally strengthened by CFRP rods lead to increase the ultimate loads by about 29%. Also, the conduct of strengthened and repaired NSM beams by CFRP rods lead to decrease the ultimate central deflection and crack widths compared to the control beam.

Muhaison, et.al (2018) [13] Carried out an experimental study on six simply supported reactive powder concrete (RPC) deep beams (with and without transverse openings) constructed for failure in shear loaded, under two equal point loads of monotonous and repeated loading. The concrete mix was made with the similar steel fiber aspect ratio but with a different volume fraction value, which is 1% or 2%. The

tested beams had the same dimensions of 1200x115x400mm for overall length, width and depth respectively and reinforced with the same amounts of main tension bars of (3 ϕ 20mm) and the same amounts of shear reinforcement (4@100 mm c/c). The experimental results show that along with the RPC, the presence of steel fiber plays a crucial role in transformation (change) the failure modes from flexural, to shear-dominated. The presence of the opening in the deep beams decay the ultimate load of the RPC specimens with volume fraction 1% under repeated load by 2.27 times. Also, there are no major variations in ultimate load values have been found between the monotonic and repeated load for different version of the solid deep beams.

2. Research significant

There are few researches about reinforced concrete deep beams under repeated loading with absolutely absents of such researches when the repeated loads combine with elevated temperature, therefore its failure mechanisms are not well understood.

3. Experimental Work

3.1 Experimental program

The experimental program consists of poured and test of six beam specimens as well as a series of control specimens (cubes, cylinders and prisms) to evaluate the mechanical properties of hardened SCC. The adopted variables include type of loading (monotonic or repeated), degree of elevated temperature (ambient temperature (20° C, 200° C and 350° C); and presence or absence of the strengthening by NSM steel bars.

3.2 Beam Specimens Description

The beam specimens have the same dimensions of 1400mm x175mm x350mm for length, width and height, respectively. The selected dimensions were imposed and compared with cross-sectional limits according to ACI 318-M14

[2]. The longitudinal reinforcements consist of ($3\phi 16\text{mm}$) steel bars with constant concrete cover of 30mm at the bottom. To ensure shear failure adopting strut and tie model of ACI 318-M14 [2], the tested beam specimens were cast and designed without stirrups to prevent bond failure of the longitudinal reinforcements, the steel bars were bent-up, with an angle of (90°), at the ends. Load control procedure with one-point load, at mid-span of an overall clear span of 1200mm, was adopted. Description and details of the tested beam specimen is shown in Table (1) and Figures (1) and (2).

Table 1. Coding and description of beams

Beam Coding	Loading Type	Elevated Temp.	Streng. by NSM
B1-M-T20	Monotonic	20° C	None
B2-R-T20	Repeated	20° C	None
B3-R-T200	Repeated	200° C	None
B4-R-T350	Repeated	350° C	None
B5-RS-T200	Repeated	200° C	Presence
B5-RS-T350	Repeated	350° C	Presence

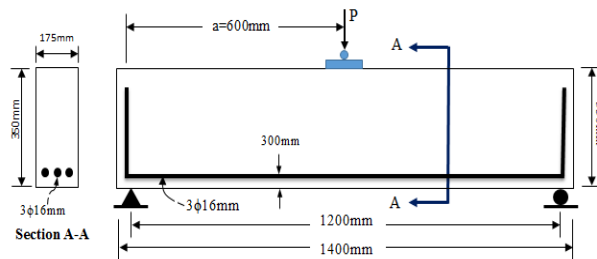


Figure 1. Beam Specimen Dimensions

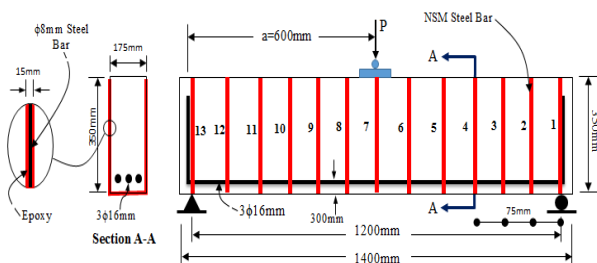


Figure 2. Details of the Tested Beam Specimens

3.3 Material

Several materials were used to prepare the beam specimen and control samples. Local production Ordinary Portland Cement (type I) meets Iraqi

standards (No.5/1984) [14]; Natural sand with the majority of particles smaller than (4.75mm) conformed to Iraqi standards (No.45/1984) [15]; Natural gravel with maximum size of (12) and conformed to Iraqi standards (No.45/1984) [15]; Fine limestone powder of size smaller than ($600\mu\text{m}$); Tap (drinking) water that is free of oils, acids, and alkalinity is appropriate for sample preparation; Superplasticizer(HRWR) admixture, "Glenium-51" conformed to ASTM C494/C494M-99a (Types F and A) [16]; Silica fume (fly ashes) conformed to ASTM C-1240 [17]; Epoxy resin (Sikadur-31) was used as grouted material to stick the NSM steel bar on burnt deep beams in strengthening stage; Two sizes (diameters) of deformed steel bars were used; ($\phi 16\text{mm}$) was used as a main reinforcement in longitudinal direction and ($\phi 8\text{mm}$) as strengthening part from the NSM steel bars technique.

3.4 Self-Compacting Concrete Mix and Pour (cast)

A rotary mixer was used to combine the raw materials and produce the self-compacting concrete (SCC). Six wooden molds made by plywood of 18mm thick and internal dimensions of 1400mm x175mm x350mm were manufactured and used to cast the deep beam specimens. It may be noted that, two of the deep beam specimens (B5-RS-T200) and (B5-RS-T350), were poured in such a way that the grooves of NSM steel bars (lateral reinforcement) was placed (extended) in the bottom and in the sides of the beams. The grooves were formed (through concrete cast) by using wooden pieces of cross-section of 15x15mm fixed at inner faces of the molds with 75mm spacing. Since the SCC is selected, no needs to any type of vibrators for concrete compaction and the fresh concrete can be poured directly in to the molds, Figure (3). It may be

noted that the SCC were selected due to narrow beam section and to ensure that the concrete flow easily at the bottom face of the beam specimens. The adopted SCC mix proportion is reported and compared with the limitation of EFNARC [18] as shown in Table (2).

Table 2. Mix proportion per (1m³)

Material	Quantity (Kg)	EFNARC [18]
Cement	400	350-600
Sand	700	< 40%
Gravel	900	< 50%
Silica Fume	25	--
L. S. P.	130	--
HRWR	10	< 2%
Water	160	-



Figure 3. Beam specimens cast

3.5 Fresh SCC Tests

According to EFNARC [18] and (ACI 237R- 07) [19], three main tests were carried out for fresh SCC mixes showing resistance to segregation, filling-ability and pass-ability. These three tests (Slump-flow by Abram's cone, V-funnel at T5 minutes and L-box) gave an indication for fresh SCC properties. Specially the important three main characteristics of the SCC (resistance to segregation, filling-ability and pass-ability). The results of the tests showed that the used SCC conforms of EFNARC [18].

3.6 Hardened SCC Tests

The compressive strength associated with concrete cubes (f_{cu}) and cylinders (f'_c) were performed at, age of (28 days), in accordance with (BS 1881-116 1983) [20] and (ASTM C39/C39M-01) [21] respectively. Splitting

tensile strength of the SCC (f_t) was achieved using standard cylindrical specimens in accordance with the ASTM C496-96[22]; the rupture test module (f_r) was carried out using 500x100x100mm prisms according to ASTM C78-02 for two-point loading [23]; The wet density of the SCC (γ_c) was measured by the average of three specimens according to (ASTM-C138) [24]. The properties listed below were stated in Table (3).

Table 3. Hardened Concrete Tests Results

Property	Value
f'_c (MPa)	44.20
Ratio of f'_c / f_{cu}	0.88
γ_c (kg/m ³)	2250
f_r (MPa)	4.35
f_t (MPa)	3.30

3.7 NSM Strengthening Technique

As mentioned before, one groove size of 15x15mm was used for NSM steel bars. After 28 days of concrete pouring, two of the burned beams that were planned to be strengthened were turned upside-down to remove the wooden strips (pieces) from the groove in the cover. Then grooves were cleaned to remove any possible dirty before introducing them into grooves; the grooves were filled to its half depth with epoxy adhesive then the steel bar was then placed in the grooves and slightly pressed, to force the epoxy to fill the space between the bars and lateral side of the groove. After positioning the steel bars, the installation was completed by adding more epoxy adhesive to fully fill the grooves and leveling the surface using a steel blade, Figure (4).



Figure 4. Strengthening by NSM Steel Bars

3.8 Instrumentation and Measurements

All beam specimens as well as the control samples, were tested for cracking and ultimate using hydraulic universal testing machine with load capacity of (300 Ton), Figure (5).



Figure 5. Beam specimens setup

Deflection was measured at the mid-span using two a dial gauge of (0.01/division) attached at the underneath faces of the tested beams. The control specimens were heated by an electric furnace (Wenger type) with internal dimensions of 500x600x750mm while, the beam specimens were heated using special heating furnace manufactured in the local market. The furnace was designed to supply only the required heating without monotonic or repeated loading.

3.9 Test Procedure

As mentioned in experimental program, five beam specimens were subjected to repeated load and one to monotonic. For monotonically loaded beam specimen (B1-M-T20), the test was performed directly up to the failure. While for the second beam specimen (B2-R-T20), the test was performed by subjecting the beam to three loading cycles, each cycle was carried out by

loading up to (230 kN) and then releasing the loads to return to the non-loading case. For the beam specimens (B3-R-T200) and (B4-R-T350), the beams were subjected firstly to an elevated temperature of (200° C) and (350° C) respectively, then to the repeated loading. On the other hand, the beam specimens (B5-RS-T200) and (B6-RS-T350) passed through three stages, subjected firstly to an elevated temperature of (200°C) and (350°C) respectively, then strengthening by NSM steel bars, and finally subjected to the repeated loading. It may be noted that, before all tests, the beam specimens were correctly prepared so that the positions of supports, applied load and dial gauges were marked at their correct positions.

4. Test results and Discussion

4.1 Effect of Loading Type on (P_{cr}) and (P_u)

The reference beam specimens (B1-M-T20) and (B2-R-T20), were tested under monotonic and repeated loads respectively in successive increments up to the failure and under repeated load with three cycles of loading. Loading Capacity is important parameter to compare between monotonic and repeated tests. The test results were provided and presented in Table (4). For the first and second beam specimens, it is observed that the first cracking load (P_{cr}) not affected by loading type, while for the other beams, no clear cracking loads were observed due to heating deformation. The ultimate load capacity (p_u) was decreased by 33% when the type of loading changed from monotonic to repeated. The loss in strength is the result of base material degradation and the loss in ability to carry load near failure when the energy dissipation in the reinforcement and Concrete decreases to the lowest level and as a result, the deformation will be increased and load capacity decreased.

Table 4. Cracking and ultimate load

Beam Coding	P_{cr} (kN)	P_u (kN)	$P_u/(P_u)_r$ (%)
B1-M-T20	78	380	-
B2-R-T20	71	255	0.67 ⁽¹⁾
B3-R-T200	-	140	0.56 ⁽²⁾
B4-R-T350	-	90	0.35 ⁽²⁾
B5-RS-T200	-	270	1.93 ⁽³⁾
B6-RS-T350	-	177	1.97 ⁽³⁾

¹with respect to (B1-M-T20).² with respect to (B2-R-T20).³ with respect to (B2-R-T200) & (B2-R-T350).

4.2 Effect of Degree of Temperature

For the burned, un-strengthened, repeatedly tested beams specimens (B3-R-T200) and (B4-R-T350), the ultimate loads were decreased to 44% and 65% respectively in comparison with the ultimate load of corresponding unheated beam specimen (B2-R-T20). This means by increasing the temperature, the ultimate load decreases because the hydrate matrix's pore size and porosity will increase, while the hydrate's mechanical properties (compressive strength and modulus of rupture) will deteriorate [25].

4.3 Effect of Strengthening on Ultimate Load

After exposed to the fire, two beam specimens, (B5-R-T200) and (B6-R-T350), were strengthened using NSM steel bars technique, and then tested under the effect of repeated loading. Tests results, Table (3), shows that the adopted strengthening technique, (NSM) steel bars, lead to increase the ultimate load by 193% and 197% for the beam specimens (B5-R-T200) and (B6-R-T350) respectively, over the control beams. This means the adopted strengthening technique enhanced the lateral strength of the tested beams and arrested the diagonal cracks to be widening as a result, the shear capacity increased.

4.4. Load-Central Deflection Relationship

Load–deflection curves of the tested beam specimens are plotted and presented in figures (6)

to (11), while, for comparison between strengthened and un-strengthened beam specimens, Figure (12) and Figure (13) are plotted. The net deflection was obtained at each stage of loading by subtracting the deflection measured by dial gauge at mid-span (reading of dial gauge 1), at each stage of loading. The testing procedure includes identifying the relationship between mid-span deflection and the applied load for each tested beam. For beam specimen (B1-M-T20) that tested under monotonic load, the load-deflection curve appears to be approximately linear along the entire path, but the line bends slightly before failure. While, Figure (7) explains this relation for (B-R-T20) that tested under repeated load with three cycles of loading. Through studying the relationship between the repeated load and deflection, it can be seen that the deflection increases with increasing the number cycles due to decreasing of beam stiffness. For the burned beam, to vanish the residual deflection, due to elevated temperature, numbers of cycle (loading-unloading) were required. It was detected that the residual deflection proportion directly with the temperature, as the temperature increases to (200 and 350°C) the residual deflections were increased compared with the non-burned beam.

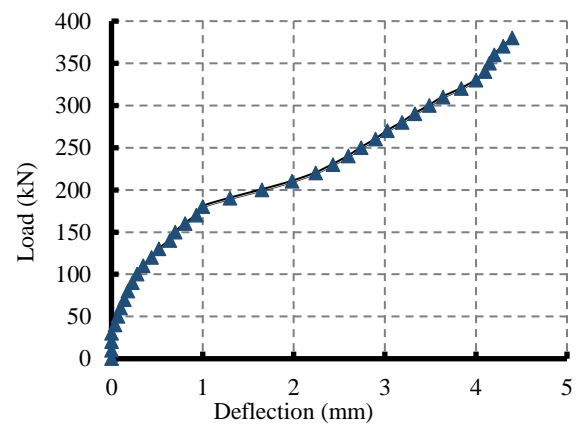


Figure 6. Load-deflection curve of the beam specimen (B1-M-T20)

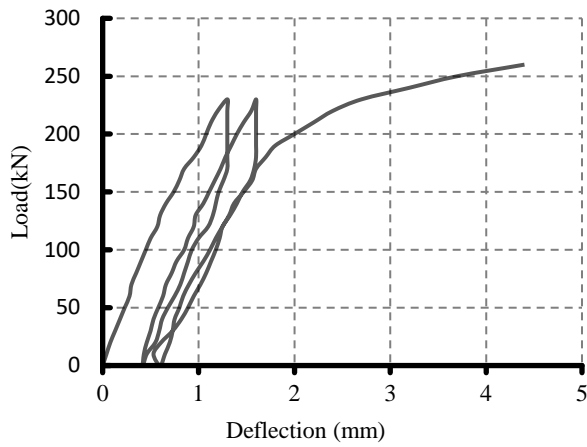


Figure 7. Load-deflection curve of the beam specimen (B2-R-T20)

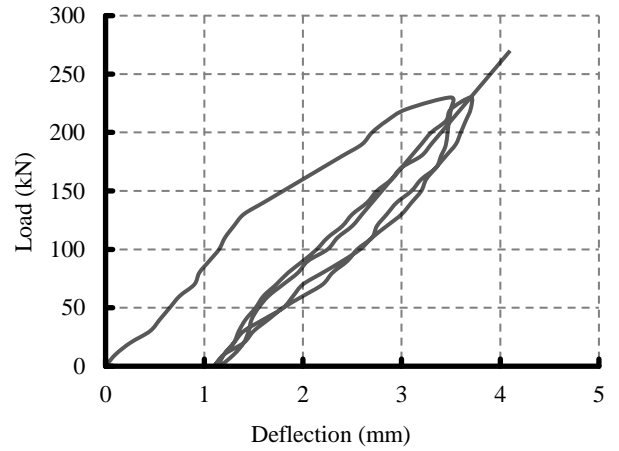


Figure 10. Load-deflection curve of the beam specimen (B5-RS-T200)

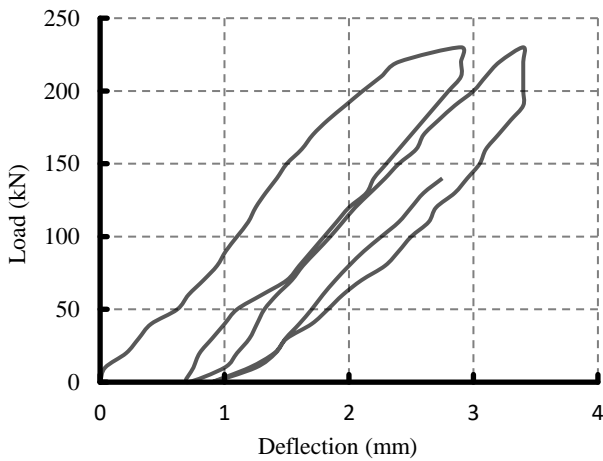


Figure 8. Load-deflection curve of the beam specimen (B3-R-T200)

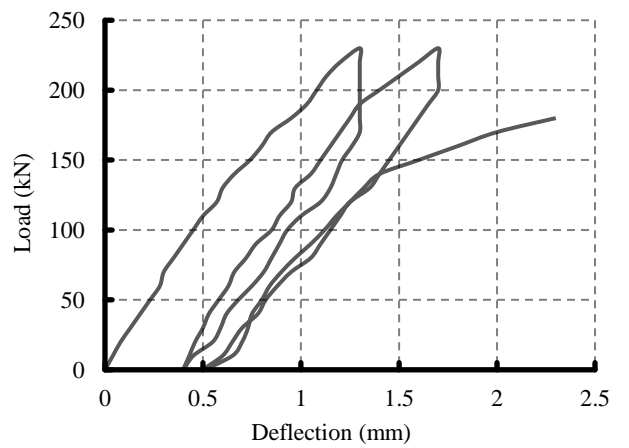


Figure 11 Load-deflection curve of the beam specimen (B6-RS-T350)

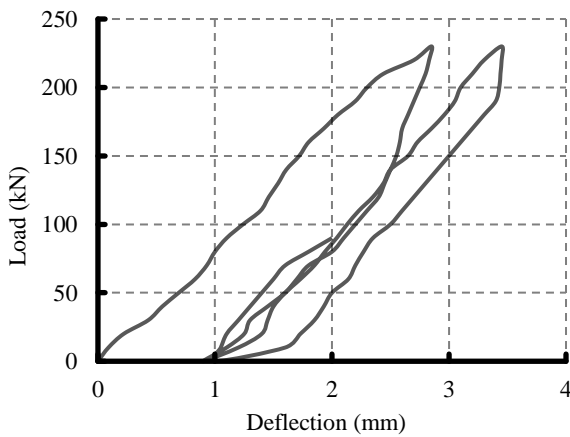


Figure 9. Load-deflection curve of the beam specimen (B4-R-T350)

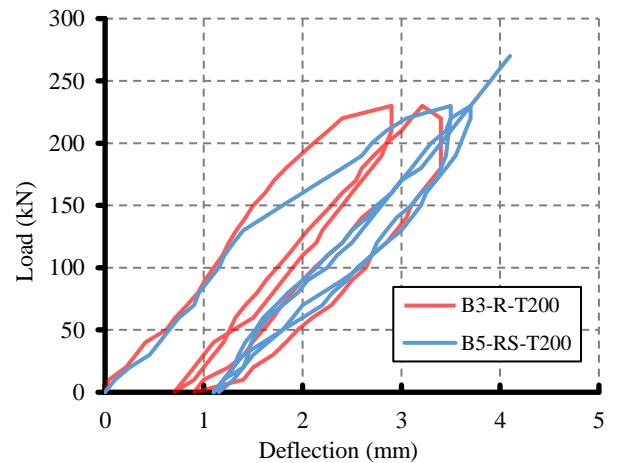


Figure 12. Load-deflection curves of the beam specimens (B3-R-T200) and (B5-RS-T200)

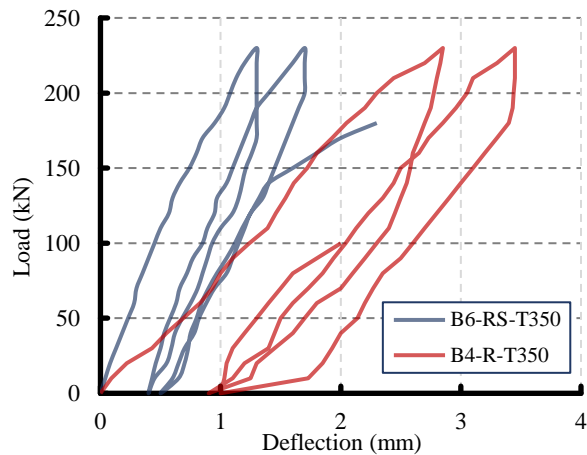


Figure 13. Load-deflection curves of the beam specimens (B4-R-T350) and (B6-RS-T350)

4.5 Crack pattern

The crack patterns, after test, are provided and shown in Figures (14) to (19). The first beam specimens was subjected to a monotonic load until failure, whereas the other beams were subjected to a repeated load. The first crack appears in the first cycle, and as the load and number of cycles increase, the width and number of the other cracks increased. Web-shear cracks occur in uncracked areas near the support where the bending moment is small and the shear force is high. They frequently occur near the inflection point or near the end supports. The angle of web-shear cracks ranges from 15 to 40 degrees. Fine extremely narrow, vertical flexural cracks were also formed, usually at the bottom face of the beam near the mid-span. As the load increased, diagonal cracks appeared suddenly and independently in one of the two shear spans. As the applied load increased, the crack began in the middle of the shear span and spread toward the support and point of load. New inclined cracks were formed parallel to the load-support direction in both shear spans. These cracks continued to spread until the beams failed. It is worth noting that, due to presence of the strengthening by NSM-steel bars, crack

formation was slowed, crack width was reduced, and crack spacing was reduced.

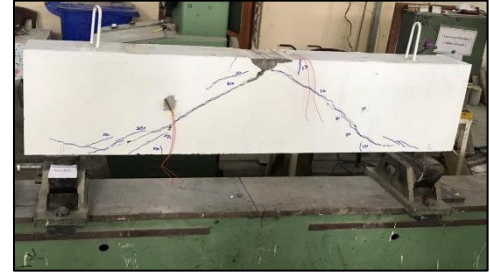


Figure 14. Crack patterns for B1-M-T20

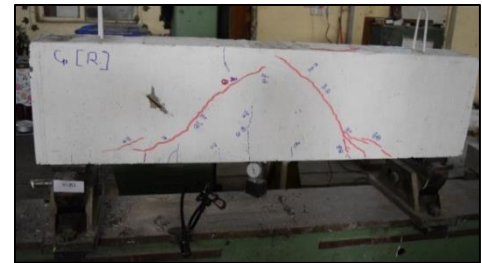


Figure 15. Crack patterns for B2-R-T20

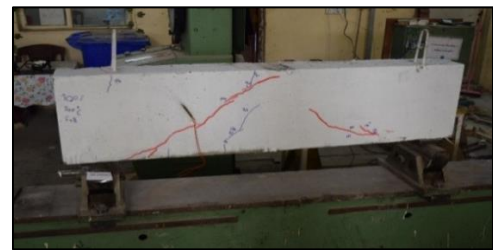


Figure 16. Crack patterns for B3-R-T200

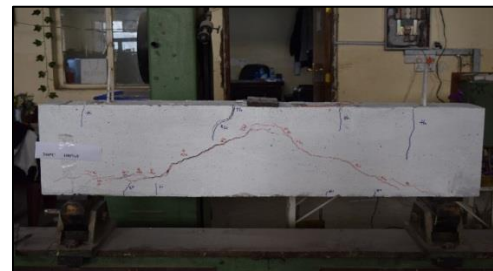


Figure 17. Crack patterns for B4-R-T350



Figure 18. Crack patterns for B5-RS-T200

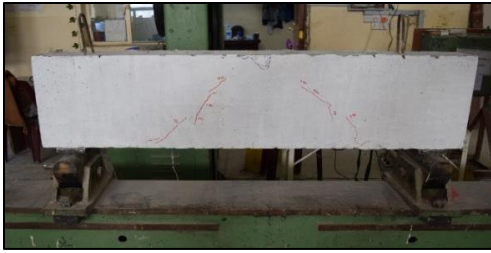


Figure 19. Crack patterns for B6-RS-T350

5. Conclusions

1. When the applied load changed from monotonic to repeated load, the ultimate load decreased by about 33%. Through repeated loading, the energy dissipation in the reinforcement and concrete decrease to the lowest level, this is the reason for high deformation and low load capacity.
2. When the degree of burning increased from 20°C to 200°C and 350°C, the ultimate load decreased by 44% and 65% respectively, in comparison with the corresponding reference beam. With raises of the degree of burning, the water in closed voids is drying rapidly leading to thermal shrinkage and as a result, the strength decreases then the ultimate load reduced (it is observed that high burning degree has inversely proportional effect on the ultimate load).
3. The adopted strengthened NSM-steel bars technique proved to be adequate to restore and increase the shear capacity of the tested beams. The ultimate load capacity were increased by 193% and 197% for the samples exposed to elevated temperature of 200°C and 350°C respectively, in comparison with reference beams. Presence of the strengthened NSM-steel bars leads to increase the lateral strength of the tested beams and arrested the diagonal cracks to be widening as a result, the shear capacity increased.

4. Presence of the NSM-steel bars leads to increase the lateral strength which means increasing of beam rigidity (stiffness) as a result, the strengthened beams show reduction in mid-span deflection compared with the reference beams (unstrengthened beams) at the same load level.

Acknowledgements

This paper is part of M.Sc. thesis that was recently completed at Civil Engineering Department, College of Engineering, Mustansiriyah University. The authors express their heartfelt gratitude to everyone who contributed, no matter how small, to the success of this study.

Conflict of Interest

The authors confirm that the publication of this article causes no conflict of interest.

6. References

1. Nilson, A. H., and Darwin, D., "Design of Concrete Structures," McGraw-Hill International Editions, 12th Edition, 1997, pp. 151.
2. ACI Committee 318, "Building Code Requirements for Structural Concrete, (ACI 318M-11) and commentary (318R-11)," American Concrete Institute, Farmington Hills, Michigan, USA, 2011, 503 pp.
3. CSA Committee A23.3-94 "Design of Concrete Structures," Canadian Standards Association, Toronto, ON, Canada, 1994, pp. 199.
4. BS 8110-1 "Structural Use of Concrete," Code of practice for design and construction, British Standards Institution, London, 1997, Part 1, pp. 26.

5. Kong F. K.,” Reinforced Concrete Deep Beams”, Tylor & Francis Books, Inc., Van Nostrand Reinhold, New York, 2002, pp.299
6. Tan K. H., Kong F. K., Teng S., Weng, L. W, “Effect of Web Reinforcement on High-Strength Concrete Deep Beams”, *ACI Structural Journal*, 1997; pp. 572-581.
7. Asplund S. O, “Strengthening bridge slabs with grouted reinforcement”, *Journal of the American Concrete Institute*, 1949, pp.397–406.
8. Broomfield J.,”The identification and assessment of defects damage and decay”, *Concrete Building Pathology*, 2003,pp.140-60
9. Aguilar G., Matamoros A. B., Parra-Montesinos G., Ramírez J.A., Wight J.K.,” Experimental evaluation of design procedures for shear strength of deep reinforced concrete beams” *American Concrete Institute*,2002, pp.539-548
10. ACI Committee 318, “Building Code Requirements for Structural Concrete (ACI 318M-99) and Commentary (318R-99),” *American Concrete Institute*, Detroit, Michigan, USA, 1999, 392 pp.13. ACI Committee
11. Heiza K. M., Meleka, N. N., and Elwkad, N. Y., “Behavior and analysis of Self-Consolidated Reinforced Concrete Deep Beams Strengthened in Shear,” *International Scholarly Research Network Civil Engineering*, Vol. 2012, pp.14.
12. Ali A., Mezher T.,” Shear strengthening of RC without stirrups for deep beams with near surface mounted CFRP rods”, *International Journal of Engineering Research and Technology*, 2015; pp.545-47.
13. 13.Muhaison S.K., Abd W.K., Alwan M.K. "Behaviour of Reactive Powder Rectangular Deep Beam with Shear Zone Opening Subjected to Repeated Load", *Journal of Engineering and Sustainable Development*. 2018,pp.77-94.
14. Iraqi Specifications No. (5), "Portland Cement", the Iraqi Central Organization for Standardization and Quality Control, Baghdad-Iraq, (1984).
15. Iraqi Specifications No. (45), "Aggregates from Natural Sources for Concrete and Building Construction", the Iraqi Central Organization for Standardization and Quality Control, Baghdad-Iraq, (1984).
16. ASTM-C494–99a, "Standard Specification for Chemical Admixtures for Concrete", *American Society for Testing and Material*, Philadelphia, USA.
17. ASTM-C1240, "Standard Test Methods for Chemical, Mass Spectrometric, and Spector Chemical Analysis of Nuclear-Grade Uranium Dioxide Powders and Pellets", *American Society for Testing and Material*, Philadelphia, USA.
18. EFNARC, "Specification and Guidelines for Self-Compacting Concrete", *Association House*, 99 West Street, Farnham, Surrey GU9, 7EN, UK. 2005; www.efca.info or www.efnarc.org.
19. ACI Committee 237. "Self-Consolidating Concrete (ACI-237 Reapproved 2007)", *American Concrete Institute*, Detroit, Michigan, USA.
20. BS 1881-116, Method for determination of compressive strength of concrete cubes, *British Standards Institute*, London, 1983.
21. ASTM C39-01, "Standard Test Method for Compressive Strength of Cylindrical Concrete Specimens", *American Society for Testing and Material*, Philadelphia, USA.
22. ASTM C496 – 96, "Standard Test Method for Splitting Tensile Strength of Cylindrical

- Concrete Specimens", American Society for Testing and Material, Philadelphia, USA.
23. ASTM C78-02, "Standard Test Method for Flexural Strength of Concrete (Using Simple Beam with Third-Point Loading", American Society for Testing and Materials, Philadelphia, USA.
 24. ASTM C138- 17, "Standard Test Method for Density (Unit Weight), Yield, and Air Content (Gravimetric) of Concrete", American Society for Testing and Material, Philadelphia, USA.
 25. Lecampion B., " A macroscopic poromechanical model of cement hydration", European Journal of Environmental and Civil Engineering, 2013.